

See discussions, stats, and author profiles for this publication at: <https://www.researchgate.net/publication/231274729>

Tailoring Porosity Development in Monolithic Adsorbents Made of KOH-Activated Pitch Coke and Furfuryl Alcohol Binder for Methane Storage†

ARTICLE *in* ENERGY & FUELS · MARCH 2010

Impact Factor: 2.79 · DOI: 10.1021/ef901536y

CITATIONS

6

READS

21

5 AUTHORS, INCLUDING:



Jacek Machnikowski

Wroclaw University of Technology

21 PUBLICATIONS 334 CITATIONS

SEE PROFILE

Tailoring Porosity Development in Monolithic Adsorbents Made of KOH-Activated Pitch Coke and Furfuryl Alcohol Binder for Methane Storage[†]

Jacek Machnikowski,^{*,‡} Krzysztof Kierzek,[‡] Krzysztof Lis,[‡] Helena Machnikowska,[‡] and Leszek Czepirski[§]

[‡]Department of Polymer and Carbonaceous Materials, Faculty of Chemistry, Wrocław University of Technology, Gdańska 7/9, 50-344 Wrocław, Poland, and [§]Faculty of Energy and Fuels, Akademia Górniczo-Hutnicza (AGH) University of Science and Technology, al. Mickiewicza 30, 30-059 Cracow, Poland

Received December 15, 2009. Revised Manuscript Received March 2, 2010

A series of microporous carbon powders of Brunauer–Emmett–Teller (BET) surface area ranging from 1900 to 2700 m²/g was made from pitch-derived semi-cokes by KOH activation at 750 °C. The powders were compacted into disk-shaped monoliths using a furfuryl-alcohol-based binder. Activation with CO₂ was used to open an access to the microporosity that was blocked by the binder char. The porous texture of monoliths was characterized by the N₂ adsorption at 77 K and mercury porosimetry, and the volumetric storage capacity and delivery V/V was determined from the methane uptake at 25 °C and 3.5 MPa. The results suggest that there is an optimum in porosity development of activated carbon powder and monolith burnoff from the point of view of the monolith performance in volumetric methane storage. The highest adsorption capacity and delivery V/V , which amount to 163 and 145, respectively, represents the monolith made of activated carbon of moderate porosity development ($S_{\text{BET}} \sim 2200 \text{ m}^2 \text{ g}^{-1}$) that was activated to the burnoff of about 10%.

1. Introduction

The increase in energy density, i.e., energy stored in a unit volume, is the key issue for a wider use of natural gas as a vehicular fuel. The theoretical and experimental studies clearly show that adsorption in porous solids under a moderate pressure can be the solution of the problem that is fully competitive to the compression under pressure of 20 MPa or cryogenic liquefaction.^{1–4}

Under supercritical conditions of operation, the methane adsorption occurs most effectively in narrow micropores. A recent study has proven the close correlation of adsorbed gas density and micropore size.⁵ The selection of a microporous high surface area activated carbon of suitable pore size distribution is, therefore, crucial for the high gravimetric adsorption capacity. According to the present knowledge, the activation with alkaline hydroxide is a method of choice for producing adsorbent with required porosity.^{4,6–8}

For any practical adsorption system made of activated carbon powder, the overall methane storage capacity comprises gas adsorbed in narrow micropores and gas compressed in meso- and macropores, which constitute interparticle voids. To enhance the volumetric storage capacity, the latter must be suppressed as much as possible. Most efforts to increase the packing density of powdered adsorbent were focused on forming monoliths with a polymer or pitch binder.^{9–13} Promising results were obtained using mechanical densification of powdered activated carbon without a binder.¹⁴ An interesting approach is the direct activation of pellets made of the mixture of an activating agent and a carbonaceous precursor.^{15,16}

The advantage of the monolithic adsorbent is convenient handling. The main drawback is a significant reduction of porosity existing in activated carbon particles because of pore blocking by the binder.^{9,11} The contribution of non-porous or poorly porous binder-derived char/coke should also be taken into account.

It seems that additional activation of baked monolith could improve accessibility to the porosity, which was blocked

[†] This paper has been designated for the special section Carbon for Energy Storage and Environment Protection.

*To whom correspondence should be addressed. Telephone: +4871-3206350. Fax: +4871-3206506. E-mail: jacek.machnikowski@pwr.wroc.pl.

(1) Parkyns, N. D.; Quinn, D. F. In *Porosity in Carbons: Characterization and Applications*; Patrick, J. W., Ed.; Edward Arnold: London, U.K., 1995; pp 293–325.

(2) Chen, X. S.; McEnaney, B.; Mays, T. J.; Alcaniz-Monge, J.; Cazorla-Amoros, D.; Linares-Solano, A. *Carbon* **1997**, *30*, 1251–1258.

(3) Cook, T. L.; Komodromos, C.; Quinn, D. F.; Ragan, S. In *Carbon Materials for Advanced Technologies*; Burchell, T. D., Ed.; Pergamon: Amsterdam, The Netherlands, 1999; pp 269–302.

(4) Lozano-Castello, D.; Alcaniz-Monge, J.; de la Casa-Lillo, M. A.; Cazorla-Amoros, D.; Linares-Solano, A. *Fuel* **2002**, *81*, 1777–2003.

(5) Alcaniz-Monge, J.; Lozano-Castello, D.; Cazorla-Amoros, D.; Linares-Solano, A. *Microporous Mesoporous Mater.* **2009**, *124*, 110–116.

(6) Lozano-Castello, D.; Cazorla-Amoros, D.; Linares-Solano, A.; Quinn, D. F. *Carbon* **2002**, *40*, 989–1002.

(7) Perrin, A.; Celzard, A.; Albinia, A.; Kaczmarczyk, J.; Mareche, J. F.; Furdin, G. *Carbon* **2004**, *42*, 2855–2866.

(8) Wu, F.-C.; Tseng, R.-L.; Hu, C.-C. *Microporous Mesoporous Mater.* **2005**, *80*, 95–106.

(9) Lozano-Castello, D.; Cazorla-Amoros, D.; Linares-Solano, A.; Quinn, D. F. *Carbon* **2002**, *40*, 2817–2825.

(10) Biloe, S.; Goetz, V.; Mauran, S. *Carbon* **2001**, *39*, 1653–1662.

(11) Kierzek, K.; Machnikowska, H.; Gryglewicz, G.; Machnikowski, J. Methane storage capacity of monoliths made of activated carbons of different porosity development. Proceedings of the 2007 International Conference on Coal Science and Technology, Nottingham, U.K., 2007; Paper 10B2.

(12) Giraldo, L.; Moreno-Pirajan, J. C. *Adsorpt. Sci. Technol.* **2009**, *37*, 255–265.

(13) Balathanigaimani, M. S.; Shim, W.-G.; Lee, J.-W.; Moon, H. *Microporous Mesoporous Mater.* **2009**, *119*, 47–52.

(14) Celzard, A.; Albinia, A.; Jasienko-Halat, M.; Mareche, J. F.; Furdin, G. *Carbon* **2005**, *43*, 1990–1999.

(15) Prauchner, M. J.; Rodriguez-Reinoso, F. *Microporous Mesoporous Mater.* **2008**, *109*, 581–584.

(16) Ramos-Fernandez, J. M.; Martinez-Escandell, M.; Rodriguez-Reinoso, F. *Carbon* **2008**, *46*, 365–389.

during monolith formation. The objective of the present work is then to assess the effect of physical activation with carbon dioxide on textural properties and performance during CH₄ storage of monoliths prepared using polyfurfuryl alcohol (PFA) as a binder. The activation behavior of monoliths made of KOH-activated carbon powders of different porosity development has been compared.

2. Experimental Section

2.1. Monolith Preparation. The raw material used in the study was semi-coke produced at a laboratory scale by carbonization at 520 °C of coal tar pitch. The activation of the semi-coke, particle size of 100–630 μm, with potassium hydroxide was performed at 750 °C for 1 h using a KOH/semi-coke ratio of 2.25:1, 3:1, and 4:1. The treatments were performed in a muffle furnace equipped with a horizontal nickel retort under nitrogen flow of 30 dm³ h⁻¹. A physical mixture of components was placed in the retort on a nickel tray. The heating rate was 10 °C min⁻¹, and the soaking time was 1 h. The reaction product was washed repeatedly with 10% solution of HCl and distilled water to remove inorganic components and, next, was dried at 110 °C for 6 h. The activated carbons produced are designated A-PC-2, A-PC-3, and A-PC-4, respectively.

The pellets of 19 mm in diameter and 7 mm in height were molded from the mixture of activated carbon and PFA, used as a binder. The proportion of binder varied from 23.0 to 33.3 wt %. PFA was added as an acetone solution to obtain a paste consistency of the mixture. The molding was performed at 160 °C under a pressure of 300 MPa. The resultant pellets were dried and then baked at 900 °C for 1 h in a horizontal tube furnace under nitrogen. The heating rate during baking was 5 °C min⁻¹, except for the critical temperature region of 300–550 °C, when the rate was reduced to 1 °C min⁻¹ to minimize the possible expansion of the pellet because of evolution of volatiles from binder decomposition.

The activation of the baked monoliths with carbon dioxide was performed at 850 °C in a horizontal tube furnace. The heating rate was 10 °C min⁻¹. The activation time was fixed experimentally to obtain the burnoff required. The baked monoliths, which are prepared from the activated carbon powders A-PC-2, A-PC-3, and A-PC-4, are designated MA-PC-2/PFA, MA-PC-3/PFA, and MA-PC-4/PFA, respectively. For the activated monoliths, the number giving a nominal burnoff or the letter A is added.

The procedure of monolith preparation follows, in principle, that of our previous work,¹¹ except the baking step was now added. It means that monoliths used in the study consist of activated carbon particles bound by rigid carbon bridges. In the former work,¹¹ the particles were joined together by cured resin, polyvinylidene fluoride (PVDF), or polyvinyl alcohol (PVA). Monoliths with acceptable mechanical properties could be produced with 10 wt % contribution of the binders; however, the surface area was reduced by about 20% compared to the initial activated carbon with a Brunauer–Emmett–Teller (BET) surface area of 2500 m² g⁻¹.

2.2. Monolith Characterization. The porosity development of the activated carbon powders and monoliths was characterized by nitrogen adsorption at 77 K in NOVA 2200, Quantachrome apparatus (p/p_0 from 0.008 to 0.98). The samples were degassed overnight at 300 °C before adsorption measurements. The adsorption data were used to determine the total pore volume (V_T), the BET specific surface area (S_{BET}), and the microporosity development in the range of 0.7–2.0 nm. The micropore volume (V_{DR}) and the average micropore width (L_0) were calculated by applying the Dubinin–Radushkevich (1) and

Stoeckli (2) equations,¹⁷ respectively, to the adsorption data up to $p/p_0 \leq 0.015$

$$V = V_{DR} \exp \left[- \left(\frac{A}{\beta E_0} \right)^2 \right]; \quad A = RT \ln \left(\frac{p_0}{p} \right) \quad (1)$$

$$L_0 = \frac{10.8}{E_0 - 11.4} \quad (2)$$

where V is the amount adsorbed at a relative pressure p/p_0 , V_{DR} is the micropore volume, A is the adsorption potential, β is the affinity coefficient (for nitrogen, $\beta = 0.33$), E_0 is the characteristic adsorption energy, and L_0 is the average micropore width.

The contribution of the micropore volume to the total pore volume was assessed as the ratio of V_{DR} to V_T (V_{DR}/V_T).

Mercury porosimetry (PASCAL 440, CE Instruments) under pressure from 0.1 to 400 MPa was used to characterize the porosity of monoliths in the diameter range from 3.6 nm to 15 μm. The characteristics measured from the relationship were bulk density d_B and apparent density d_A , measured under pressures of 0.1 and 400 MPa, respectively, total pore volume (V_{tot}), volume of mesopores of size 3.6–50 nm ($V_{<50}$), and volume of pores larger than 50 nm ($V_{>50}$).

The particle size distribution of activated carbon powders was measured in water by a Malvern Mastersizer 2000 (632 nm laser), with a drop of surfactant added to improve wettability (Figure 1).

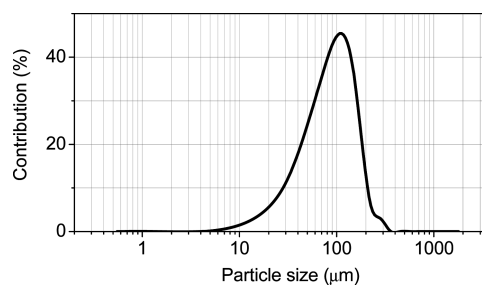


Figure 1. Particle size distribution of activated carbon A-PC-3.

Methane adsorption isotherms were measured under pressure up to 7 MPa using a homemade high-pressure volumetric apparatus.¹⁸ The amount of methane (mmol g⁻¹) adsorbed at 3.5 MPa was used to calculate volumetric storage capacity (V/V_A). The delivered capacity (V/V_D) was calculated as a difference between (V/V_A) and the storage capacity at the release pressure (0.1 MPa). Three monoliths were typically used in an individual measurement, so that the storage capacity should be considered as an average for a given series.

Commercial granular activated carbon Norit R2 was used as a reference material in methane adsorption measurements.

3. Results and Discussion

3.1. Characterization of Activated Carbon Powders. Table 1 gives the characteristics of porosity in powdered activated carbons A-PC-2, A-PC-3, and A-PC-4. As expected, the increase in the KOH/PC ratio from 2.25:1 to 4:1 results in more developed porosity. The increases in the pore volume

Table 1. Characteristics of Porous Texture for Activated Carbon Powders Determined from N₂ Adsorption Isotherms at 77 K

activated carbon	S_{BET} (m ² g ⁻¹)	V_T (cm ³ g ⁻¹)	V_{DR} (cm ³ g ⁻¹)	L_0 (nm)	V_{DR}/V_T
A-PC-2	1920	0.785	0.633	1.12	0.81
A-PC-3	2230	0.964	0.725	1.25	0.75
A-PC-4	2690	1.176	0.822	1.36	0.70

(17) Stoeckli, F.; Daguerre, E.; Guillot, A. *Carbon* **1999**, 37, 2075–2077.

(18) Czepirski, L.; Hołda, S.; Łaciak, B.; Wójcikowski, M. *Adsorpt. Sci. Technol.* **1996**, 14, 77–82.

and the BET surface area are associated with a widening of pores as reflected by a larger average micropore size L_0 and a lower contribution of the micropore volume to the total pore volume V_{DR}/V_T . However, all of the activated carbon are basically microporous.

3.2. Monoliths Preparation. The activated carbon most widely studied was A-PC-3 with a BET surface area of about $2200 \text{ m}^2 \text{ g}^{-1}$. The selection of this material resulted from our previous work, which showed the maximum of V/V_T for monoliths made of activated carbon of moderate porosity development.¹¹ Relatively high binder proportion in the pressed mixture (33.3 wt %) ensures that pellets of high mechanical strength could be produced with a good repeatability. Samples A-PC-2 and A-PC-4 with S_{BET} of about 1900 and $2700 \text{ m}^2 \text{ g}^{-1}$, respectively, were used to assess the effect of porosity development in activated carbon powder on monolith properties. In the case of these materials, the proportion of PFA was reduced to a minimum, which was necessary to press compact pellets, i.e., 23 and 28.6 wt %, respectively.

Table 2 summarizes essential data, which characterize manufacturing of monoliths from A-PC-3, A-PC-2, and A-PC-4. The content of binder char in monolith was estimated taking into account the weight losses during PFA curing and subsequent carbonization and activated carbon annealing at 900°C . The shape density of a baked monolith was assessed as its mass divided by volume, which was calculated on the basis of geometrical dimensions (diameter and height) and assuming cylindrical shape. The shape density of monoliths varies from 0.71 to 0.59 g cm^{-3} in dependence upon both the porosity of activated carbon and binder char proportion. The value of about 0.7 g cm^{-3} can be regarded as quite satisfactory.

Table 2. Properties of Baked and Activated Monoliths

monolith symbol	binder content (wt %)	activation time (h)	burnoff (wt %)	shape density (g cm^{-3})	density lost (g cm^{-3})
MA-PC-3/PFA	18.7			0.69	
MA-PC-3/PFA-10		2.0	10.0	0.62	0.07
MA-PC-3/PFA-15		3.5	15.5	0.59	0.10
MA-PC-2/PFA	13.5			0.71	
MA-PC-2/PFA-A		1.5	12.6	0.62	0.09
MA-PC-4/PFA	17.0			0.59	
MA-PC-4/PFA-A		1.5	7.5	0.55	0.04

A preliminary activation study with MA-PC-3/PFA showed that 20 wt % is a limit of weight loss in terms of monolith integrity. On the basis of this experiment, the activation time for this series was set to 2 and 3.5 h to obtain burnoffs of about 10 and 15 wt %. For MA-PC-2/PFA and MA-PC-4/PFA, the nominal burnoff was 10 wt %; however, that gained was 12.6 and 7.5 wt %, despite the same activation time (1.5 h). The reason for a higher reactivity toward CO_2 of the former monolith is not clear. In all cases, the activation results in a considerable decrease in the shape density, with the extent being proportional to the burnoff.

3.3. Porous Texture of Monoliths. N_2 adsorption isotherms at 77 K (Figure 2) reveal a drastic reduction of the nitrogen adsorption capacity of baked monoliths compared to corresponding activated carbon powders. Activation allows us to recover a part of the lost porosity. It is interesting to note that both baked and activated monoliths preserve the specific microporous character of the initial activated carbon. The exception is MA-PC-4/PFA, with the differentiated isotherm profiles for individual monoliths (Figure 2c). Most of them are characterized by the enhanced adsorption capacity at

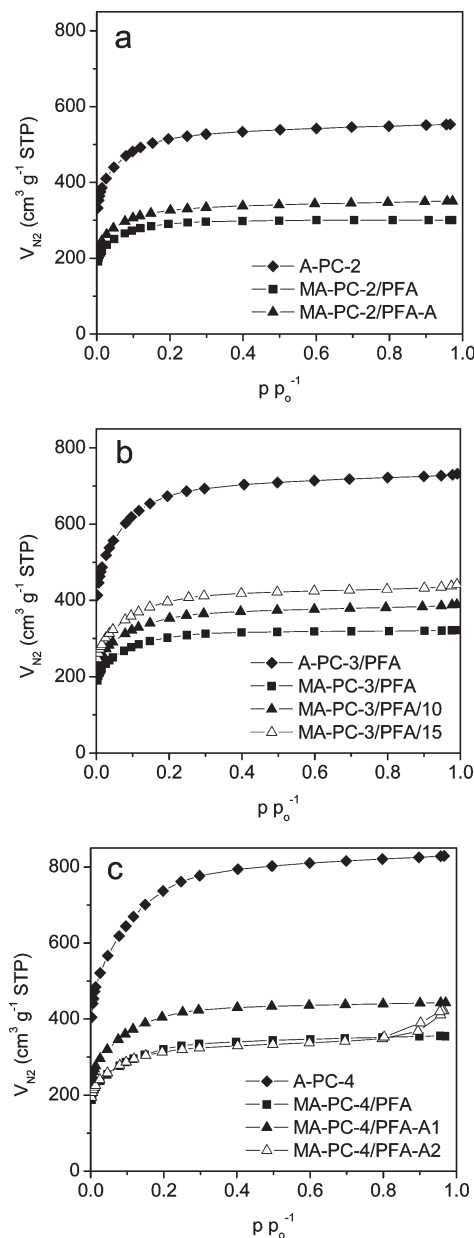


Figure 2. Isotherms of N_2 adsorption at 77 K of activated carbon powder and monolith for the series (a) A-PC-2, (b) A-PC-3, and (c) A-PC-4.

p/p_0 above 0.8. The unusual widening of pores can be attributed to burning out of thin pore walls of that superporous activated carbon.

Table 3 gives porous structure parameters calculated from N_2 adsorption isotherms. The results show the reduction of the surface area S_{BET} and micropore volume V_{DR} of monoliths compared to the corresponding activated carbon powder by about 50% and near 60% for MA-PC-4/PFA. The porosity loss has to be induced mostly by pore blocking, occurring to the extent that is independent of the binder char content. Activation allows for a partial opening of the blocked porosity, apparently without the widening of pores. The most porous texture, S_{BET} near $1500 \text{ m}^2 \text{ g}^{-1}$ and V_{DR} about $0.47 \text{ cm}^3 \text{ g}^{-1}$, is reported for MA-PC-3/PFA-15, i.e., the monolith of highest binder char content that was activated to the burnoff of ~ 15 wt %. It means an increase in the porosity by 25% compared to the baked monolith.

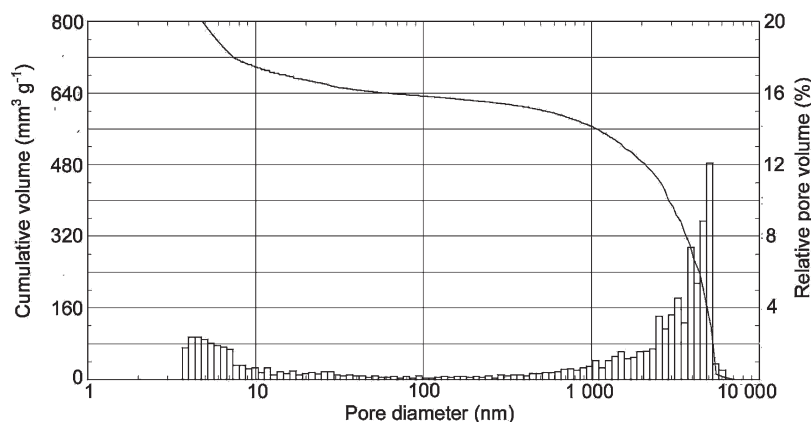


Figure 3. Pore size distribution for the monolith MA-PC-3/PFA.

Table 3. Characteristics of Porous Texture for Activated Carbon Monoliths Determined from N₂ Adsorption Isotherms at 77 K

monolith symbol	S_{BET} (m ² g ⁻¹)	V_{T} (cm ³ g ⁻¹)	V_{DR} (cm ³ g ⁻¹)	L_0 (nm)	$V_{\text{DR}}/V_{\text{T}}$
MA-PC-3/PFA	1180	0.490	0.385	1.26	0.79
MA-PC-3/PFA-10	1300	0.553	0.425	1.17	0.77
MA-PC-3/PFA-15	1470	0.627	0.472	1.20	0.75
MA-PC-2/PFA	1000	0.384	0.331	1.20	0.86
MA-PC-2/PFA-A	1170	0.469	0.397	1.26	0.84
MA-PC-4/PFA	1180	0.505	0.374	1.32	0.74
MA-PC-4/PFA-A1	1470	0.621	0.470	1.35	0.75
MA-PC-4/PFA-A2	1170	0.596	0.386	1.29	0.65
Norit R2	1280	1.074	0.469	n.d.	0.44

In relation to different profiles of N₂ adsorption isotherms measured for individual monoliths made of A-PC-4, two sets of porosity parameters are given in Table 3. The inconsistency in activation behavior can reflect a difference in the porous texture. The practical conclusion from the observation is that, for extremely porous activated carbons and a limited amount of binder, the activation process can hardly be controlled.

Figure 3 is a histogram showing the pore size distribution measured using mercury porosimetry for the monolith MA-PC-3/PFA. The bimodal distribution of meso- and macropores is characteristic of all baked and activated monoliths. The first maximum is located in the mesopore region and indicates existence of pores with diameters up to 10 nm. This porosity seems to be related in part to the porous texture of activated carbon particles. A much stronger second maximum covers a wide range of pore diameters from about 400 to 6000 or even 8000 nm. The macropores represent interparticle voids created because of a limited compaction during molding with the binder. The contribution of pores created because of binder decomposition on baking cannot be neglected.

Table 4 gives properties of monoliths that were calculated from mercury porosimetry measurements. The data show the highest values of bulk density d_{B} and apparent density d_{A} for MA-PC-2/PFA but a minimum of the pore volume for MA-PC-3/PFA. This apparent discrepancy can be easily understood when keeping in mind essential differences between the monoliths in porosity of constituting activated carbon and binder char contribution. Because MA-PC-3/PFA is made of more porous activated carbon, the particles have lower apparent density but the interparticle voids are reduced as a result of enhanced binder content (lower $V_{>50}$).

Bulk density d_{B} that is measured at the pressure of 0.1 MPa corresponds to the frame including pores smaller than

15 000 nm. In general, d_{B} values are higher by about 0.02–0.04 g cm⁻³ than shape density, given in Table 2. A larger gap between d_{B} and shape density for MA-PC-4/PFA proves the presence of pores larger than 15 000 nm, which mercury can penetrate.

Activation results in a considerable decrease in densities, in particular d_{B} , and an increase in surface area S and pore volume in both the range of mesopores $V_{<50}$ and macropores $V_{>50}$. For baked monoliths, the contribution of mesopores in the total pore volume V_{tot} varies from 13 to 25% with an increasing porosity of activated carbon. Except for MA-PC-4/PFA, the activation enhances the contribution of mesopores. The textural characteristics confirm an inconsistent behavior on the activation of individual monoliths made of A-PC-4.

3.4. Methane Storage Capacity. Figure 4 gives isotherms of methane adsorption at 25 °C for monoliths and commercial NORIT activated carbon under pressure up to 6 MPa. The estimations at 3.5 MPa show that gravimetric methane uptake varies from 6.7 to 10.2 mmol g⁻¹ and the volumetric storage capacity covers the range of 112–163 (Table 5). In most cases, the activation considerably enhances amount of methane stored on both the gravimetric and volumetric basis. Taking into account a moderate microporosity development, the performance of monoliths can be considered as quite satisfactory. In fact, it is higher than could be anticipated on the basis of some literature data.^{4,19} A 2-fold explanation of the phenomenon can be proposed. First, it seems that, for monoliths, the data from adsorption of

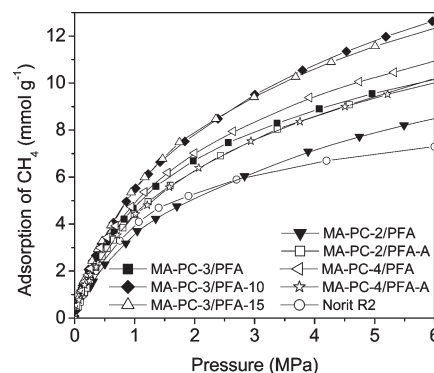


Figure 4. Methane adsorption isotherms at 25 °C on baked and activated monoliths.

(19) Sun, Y.; Liu, C.; Su, W.; Zhou, Y.; Zhou, L. *Adsorption* 2009, 15, 133–137.

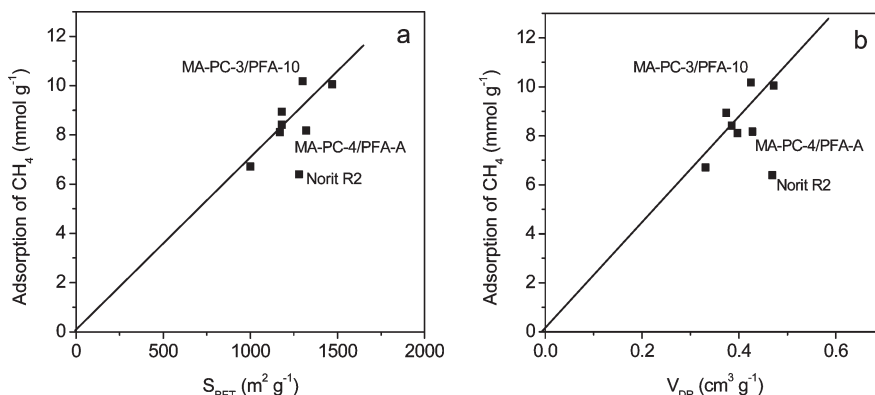


Figure 5. Relationship between the methane uptake and (a) BET surface area and (b) micropore volume of baked and activated monoliths.

Table 4. Density and Porosity of Monoliths Determined Using Mercury Porosimetry

monolith symbol	d_B (g cm ⁻³)	d_A (g cm ⁻³)	S (m ² g ⁻¹)	V_{tot} (cm ³ g ⁻¹)	$V_{<50}$ (cm ³ g ⁻¹)	$V_{>50}$ (cm ³ g ⁻¹)
MA-PC-3/PFA	0.712	1.126	49.3	0.518	0.088	0.430
MA-PC-3/PFA-10	0.656	1.112	69.2	0.624	0.120	0.504
MA-PC-3/PFA-15	0.623	1.086	90.3	0.672	0.140	0.532
MA-PC-2/PFA	0.753	1.364	63.8	0.571	0.076	0.496
MA-PC-2/PFA-A	0.662	1.292	88.3	0.736	0.141	0.594
MA-PC-4/PFA	0.686	1.165	98.0	0.604	0.154	0.450
MA-PC-4/PFA-A1	0.593	1.123	113.4	0.794	0.177	0.616
MA-PC-4/PFA-A2	0.528	1.255	116.8	1.075	0.245	0.830

Table 5. Gravimetric and Volumetric Methane Capacities at 25 °C and 3.5 MPa for Baked and Activated Monoliths

monolith symbol	uptake		delivery (V/V_D)
	mmol g ⁻¹	(V/V_A)	
MA-PC-3/PFA	8.41	146	128
MA-PC-3/PFA-10	10.18	163	145
MA-PC-3/PFA-15	10.05	153	134
MA-PC-2/PFA	6.71	123	109
MA-PC-2/PFA-A	8.11	131	116
MA-PC-4/PFA	8.94	150	134
MA-PC-4/PFA-A	8.17	112	102
Norit R2	6.39	99	90

nitrogen at 77 K underestimate the development of microporosity, which is accessible for methane uptake at 25 °C at elevated pressure. A similar behavior has already been reported for resin carbon beads and discs.²⁰ Second, the contribution of narrow mesopores of width of 2–3 nm to the capacity of monoliths cannot be neglected.¹⁴ This category of mesopores is most abundant in KOH-activated carbons.^{14,21}

According to earlier reports,^{4,7,19} the methane uptake at 3.5 MPa should be proportional to the BET surface area and micropore volume determined by nitrogen adsorption at 77 K. For materials of this study, the relationships show some discrepancies from the trend (Figure 5). An exceptionally good performance, with the uptake of 10.2 mmol g⁻¹ and the adsorption capacity/delivery of 163 and 145, respectively, represents MA-PC-3/PFA-10 with a rather moderate S_{BET} (1300 m² g⁻¹) and V_{DR} (0.425 cm³ g⁻¹). We suppose that the monolith combines suitable microporosity with acceptable packing density. However, a more detailed porosity characterization is needed to support this view.

A lower than anticipated capacity concerns commercial activated carbon and monolith of heterogeneous porous texture (MA-PC-4/PFA-A). A distinctly worse performance of Norit R2 compared to monoliths supports the meaning of

pore structure peculiarities, as discussed above. Non-uniform activation throughout the monolith, deeper in the outer compared to the inner part, can also contribute to the worse performance of some activated monoliths. This observation suggests that the extent of burnoff must be individually and carefully adjusted to the monolith composition to avoid “overactivation”.

4. Conclusions

Monolithic adsorbents of acceptable packing density and mechanical strength were successfully produced using molding of powdered activated carbon produced by KOH activation of pitch semi-coke with PFA binder followed by baking at 900 °C. However, the BET surface area and micropore volume of monolith is reduced by about 50% compared to the original activated carbon because of pore blocking by binder-derived char.

The activation with CO₂ can be used to restore in part the microporosity existing in activated carbon particles that is blocked by binder char. The extent of the burnoff must be individually adjusted to the monolith composition to avoid micropore widening and the excess of density loss because of interparticle void generation.

The highest volumetric adsorption capacity and the delivery V/V at 25 °C and 3.5 MPa, which amount to 163 and 145, respectively, represents the monolith made of activated carbon of moderate porosity development ($S_{BET} \sim 2200$ m² g⁻¹) that was activated to the burnoff of about 10%. The satisfactory performance is the effect of compromise between sufficient microporosity development ($S_{BET} = 1300$ m² g⁻¹, and $V_{DR} = 0.43$ cm³ g⁻¹) and acceptable packing density ($d_B = 0.66$ g cm⁻³).

Acknowledgment. The financial support provided by the Ministry of Science and Higher Education, Poland, Project PBZ-MEiN-2/2/2006, is gratefully acknowledged.

(20) Alain, E.; McEnaney, B. *Adsorpt. Sci. Technol.* **2005**, *23*, 573–584.

(21) Kierzek, K.; Frackowiak, E.; Lota, G.; Grylewicz, G.; Machnikowski, J. *Electrochim. Acta* **2004**, *49*, 515–523.